Active Feedback Control of Turbulent Pipe Flow

Koji Fukagata [1, 2] and Nobuhide Kasagi [1]
[1] *Department of Mechanical Engineering, The University of Tokyo*
7-3-1 Hongo, Bunkyo-ku, Tokyo 113-8656, Japan
[2] *Institute for Energy Utilization, AIST*
1-2-1 Namiki, Tsukuba-shi, Ibaraki 305-8564, Japan
fukagata@thtlab.t.u-tokyo.ac.jp

Active feedback control of turbulent pipe flow is studied by means of direct numerical simulation (DNS). First, the active cancellation control proposed by Choi et al. (1994) is tested in the DNS of turbulent pipe flow at low Reynolds numbers. The drag reduction rate attained by this control is found to be almost the same as in the case of turbulent channel flow. Then, the control is applied only partially over a limited length in the streamwise direction. The upstream control effect remains over a distance of about $2000 - 2500$ wall units downstream of the point where the control is terminated.

1. Introduction

In order to realize an active feedback control system for turbulent flow, different components consisting such system, i.e., sensor, actuator, controller and control algorithm, should be developed simultaneously. Among these, the control algorithm has been mainly developed and assessed by using direct numerical simulation (DNS) of controlled turbulent flow fields. Choi et al. (1994) attained considerable drag reduction in their DNS of turbulent channel flow at low Reynolds numbers by blowing and suction, of which velocity, v_w, is determined so as to oppose the velocity components induced by the near-wall quasi-streamwise vortices (QSVs). Although their study assumed a highly idealized situation, later studies (Lee et al., 1998; Endo & Kasagi, 2000; Iwamoto et al., 2002) demonstrated that the above active cancellation strategy proposed by Choi et al. (1994) should be effective even for the drag reduction in more practical situations.

Most of the previous studies have dealt with plane channel flows, while a flow in a circular pipe is another canonical wall-bounded flow and its control has several direct practical applications such as drag reduction in gas / petroleum pipeline. Control of pipe flow by rotation (Orlandi & Fatica, 1997) and by oscillation around its axis (Quadrio & Sibilla, 2000) has been reported with some degree of success. However, more widely applicable wall actuation control mentioned above should be tested in pipe flows. It would also be interesting to explore if the control algorithm proposed for channel flow is also valid for pipe flow. Therefore, in the first part of the present study, an active control algorithm is applied to a turbulent pipe flow. Here, we mainly focus on the overall control performance and provide data useful for a feasibility study of real control systems.

In reality, it may not be possible both technologically and financially to have an entire wall surface equipped with an array of active feedback control units. In many perspective cases,

the number of actuators / sensors should be limited. In the previous DNS studies, however, the control has always been assumed on the entire surface, so that the knowledge on spatially inhomogeneous control is lacking. The second part of the present study is therefore devoted to a control only applied on a limited wall surface area. DNS is carried out by dividing the computational domain into two and the control is applied only in the upstream sub-region of a pipe.

2. Numerical method

A computational code for DNS of turbulent pipe flow was developed based on a second-order accurate finite difference scheme on the cylindrical coordinate system. A special care was paid for consistency in the discretized space so that the energy is conserved by the inviscid part of the governing equation (Fukagata & Kasagi, 2002a). The time integration was advanced by using the third order accurate Runge-Kutta / Crank-Nicolson (RK3/CN) scheme. The statistics of an uncontrolled flow at $Re_\tau = u_\tau R/\nu = 180$ ($Re_b = 2U_b R/\nu \simeq 5300$) computed by using the present code were in excellent agreement with previous DNS data by Eggels et al. (1994).

Throughout the present work, the mass flow rate, i.e., the bulk mean velocity U_b was kept constant. A fully developed turbulent flow is assumed in a circular pipe of a radius R, but the computation is made in a pipe of finite length L ($L = 35 - 40R$ in the present study) with periodic boundary conditions at both ends. Thus, strictly speaking, the flow field should be always periodic in the streamwise direction, and it is particularly so in the case of partial area control.

The control algorithm used in the present study is so-called active cancellation control (v-control) of Choi et al. (1994), i.e.,

$$v_w = -u_r(y_d) \ . \tag{1}$$

Here, y_d denotes the distance between wall and a virtual detection plane as shown in Figure 1, and v_w is the radial velocity at the wall, i.e., $v_w = u_r|_{r=R}$.

3. Results

The investigation is initiated with active cancellation control applied on the entire wall with different locations of the detection plane, $y_d^+ = (R-r)^+ = 5$, 10, 15 and 20. Hereafter, superscript $+$ is used for the dimensionless quantity normalized by the friction velocity of uncontrolled flow and the kinematic viscosity. Simulations were performed for two relatively low Reynolds numbers, $Re_b = 3050$ ($Re_\tau \simeq 110$) and $Re_b = 5300$ ($Re_\tau \simeq 180$). It should be noted that in the case of $Re_b = 3050$ low-frequency intermittency was observed, which suggested that the flow remained in a transitional slug flow region. Statistics shown below were obtained from the data accumulated over approximately 2000 wall unit time-span after the flow was judged to be in a quasi-steady state.

Figure 2 summarizes the relationship between y_d^+ and the drag reduction rate, $R_D = (C_{f0} - C_f)/C_{f0}$, where C_{f0} is the skin friction coefficient of the uncontrolled flow. Corresponding data for channel flow reported by Choi et al. (1994) are also plotted. The dependency of R_D on y_d^+ is similar to that in the channel flow. The maximum drag reduction is attained at $y_d^+ = 15$ for both Reynolds numbers presently specified. The magnitude of drag reduction rate is also comparable to that in the channel despite that the controlled surface area per volume of a pipe is twice as

large as that of a channel.

From the practical point of view, it is of great importance to investigate the net power saving achieved by an active feedback control system. To do this, one should assume the efficiency of the hardware components. In the present study, a total efficiency, η, is defined as $\eta = W_a/(W_a + Q_a + Q_s + Q_c)$ where W_a is the power input from actuator to flow, and Q_a, Q_s and Q_c denote the power dissipation in actuators, sensors and controllers, respectively. Figure 3 shows the sum of power input required to drive the flow and that needed to operate the active feedback control system, i.e., $W_{tot} = W_p + W_a/\eta$. These curves have been normalized by the driving power for uncontrolled flow, W_{p0}, and plotted as functions of η with different values of y_d^+. It is, of course, natural that the rate of net power saving becomes poorer with the decrease of η. Especially, one cannot secure net power saving with $\eta < 0.01$ (i.e. less than 1 % efficiency) regardless of the choice of y_d^+. This seems to be a quite severe criterion for a real system, in which, for example, electromagnetic actuators of relatively high power dissipation are used.

Fundamental statistics of velocity and pressure are also accumulated. As examples, mean and RMS levels of velocity are shown in Figure 4. Changes in these statistics due to control are found to be similar to those in the channel flow.

Simulation is continued with control applied only in the region of $0 < z < L_c$ as shown in Figure 5. Hereafter, only the case of $Re_b = 5300$ is considered and the detection plane is fixed at $y_d^+ = 10$. The separation length, L_s, is identical to the computational domain length, i.e. $L_s^+ = L^+ = 7360$.

Figure 6 shows the drag reduction rate, R_D, as a function of L_c^+. Computed reduction rate is nearly proportional to the ratio of control length to separation length, i.e., $R_D \simeq (L_c/L_s)R_{D1}$, where R_{D1} is the drag reduction rate with control on entire wall. This result can be explained by the behavior of the local skin friction coefficient, $C_f(z)$, plotted in Figure 7. The common behavior observed regardless of the value of L_c is as follows. In the controlled region, $C_f(z)$ decreases following a single curve. Just after the control ends, say in the region of $L_c^+ < z^+ < L_c^+ + 60$, the skin friction rapidly increases. Subsequently, $C_f(z)$ increases almost linearly up to the level of the uncontrolled flow. The endurance length of control effect after the end point of control is $2000 - 2500$ wall units. In addition to production of the Reynolds shear stress accompanied by re-generation of vortices as shown in Figure 8, anomalous pressure-strain correlation is found to cause the rapid increase of $C_f(z)$ right downstream of the end point of control (Fukagata & Kasagi, 2002b).

4. Conclusions

Active cancellation control was applied to DNS of turbulent pipe flow. From the simulation with control on entire and partial surface, we found:

1. The maximum drag reduction rate is comparable to that of channel flow (~ 25 %);
2. At least, a total device efficiency more than 1 % is required for a real active feedback control system to attain meaningful net power saving;
3. Even if the control is not applied on an entire surface, the drag reduction nearly proportional to the area of control can be obtained;

4. The flow recovers to the uncontrolled state about $2000 - 2500$ wall unit length downstream of the end point of control.

References

Choi H., Moin P. and Kim J., 1994. Active turbulence control for drag reduction in wall bounded flows. *J. Fluid Mech.* **262**, 75-110.

Eggels J.G.M., Unger F., Weiss M.H., Westerweel J., Adrian R.J., Friedrich R. and Nieuwstadt F.T.M., 1994. Fully developed turbulent pipe flow: a comparison between direct numerical simulation and experiment. *J. Fluid Mech.* **268**, 175-209.

Endo T. and Kasagi N., 2000. Feedback control of wall turbulence with wall deformation. *Int. J. Heat Fluid Flow* **21**, 568-575.

Fukagata K. and Kasagi N., 2002a. Highly energy-conservative finite difference method for cylindrical coordinate system. *J. Comput. Phys.*, submitted.

Fukagata K. and Kasagi N., 2002b. Active control for drag reduction in turbulent pipe flow. *5th Conf. on Engineering Turbulence Modelling and Measurement (ETMM5), Mallorca, Spain, 16-18 September 2002*, to be presented.

Iwamoto K., Suzuki Y. and Kasagi N., 2002. Reynolds number effect on wall turbulence: Toward effective control. *Int. J. Heat Fluid Flow*, to appear.

Lee C., Kim J. and Choi H., 1998. Suboptimal control of turbulent channel flow for drag reduction. *J. Fluid Mech.* **358**, 245-258.

Orlandi P. and Fatica M., 1997. Direct simulations of turbulent flow in a pipe rotating about its axis. *J. Fluid Mech.* **343**, 43-72.

Quadrio M. and Sibilla S., 2000. Numerical simulation of turbulent flow in a pipe oscillating around axis. *J. Fluid Mech.* **424**, 217-241.

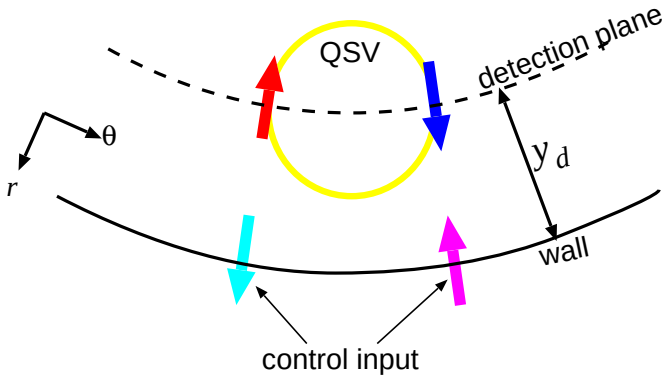

Figure 1 : Active cancellation control in pipe.

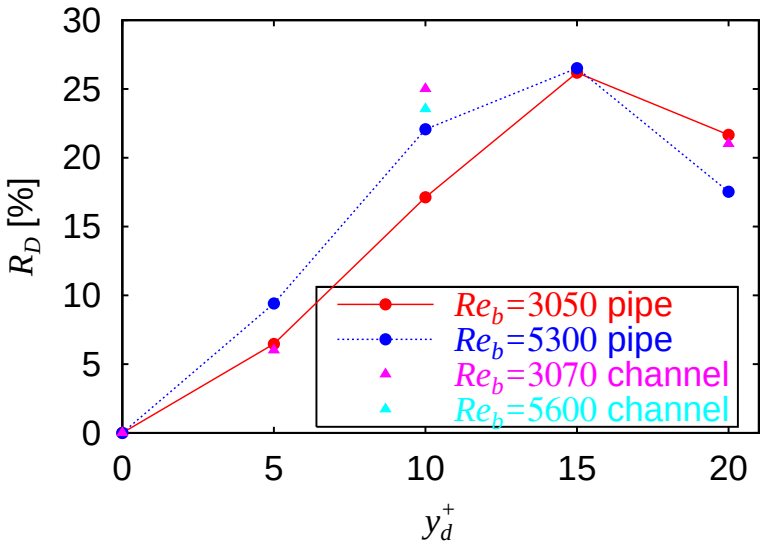

Figure 2: Drag reduction rate, R_D.

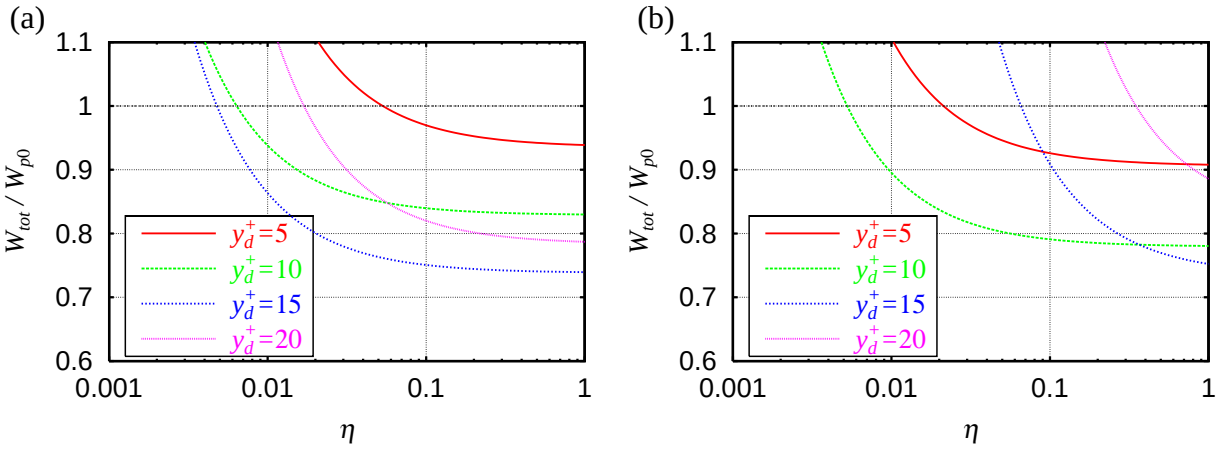

Figure 3 : Total power saving ratio as functions of system hardware efficiency. (a) $Re_b = 3050$; (b) $Re_b = 5300$.

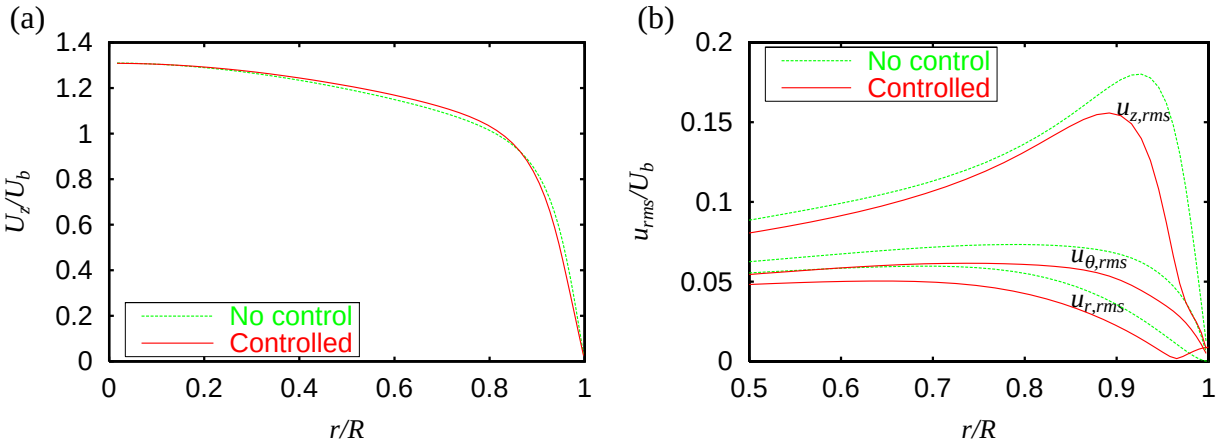

Figure 4 : Velocity statistics of controlled flow at $Re_b = 5300$, $y_d^+ = 10$. (a) Mean velocity; (b) RMS level of velocity fluctuations.

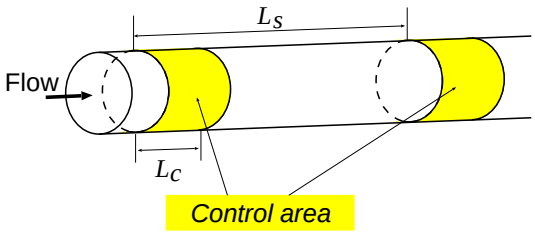

Figure 5: Schematic of partial control.

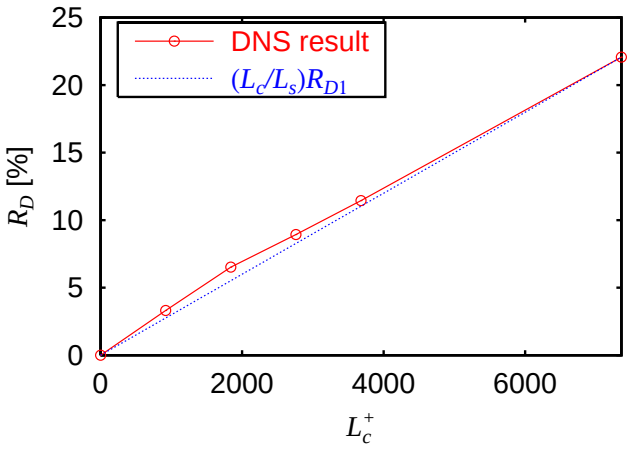

Figure 6: Drag reduction rate as a function of control length.

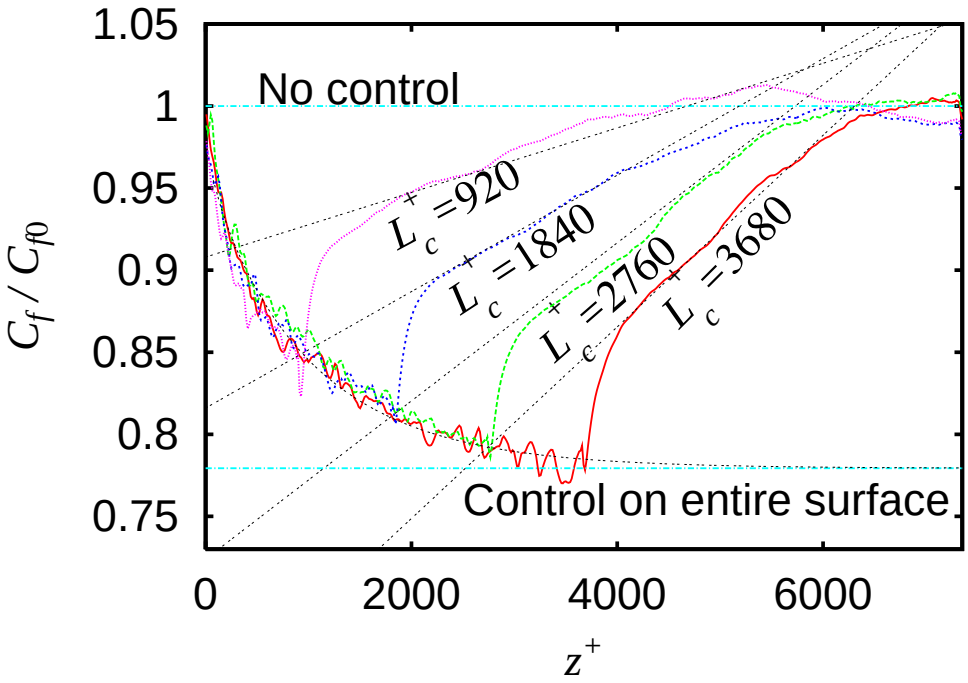

Figure 7: Normalized local skin friction coefficient, for different control length.

(a)

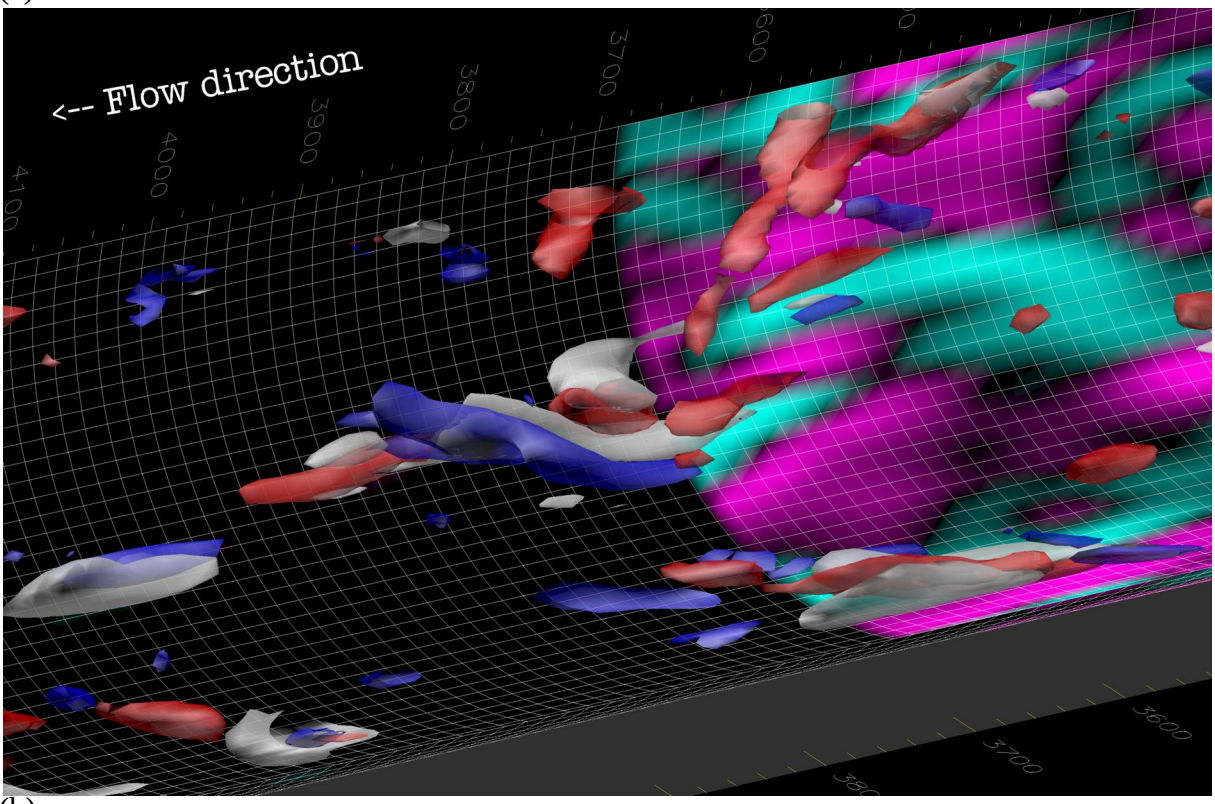

(b)

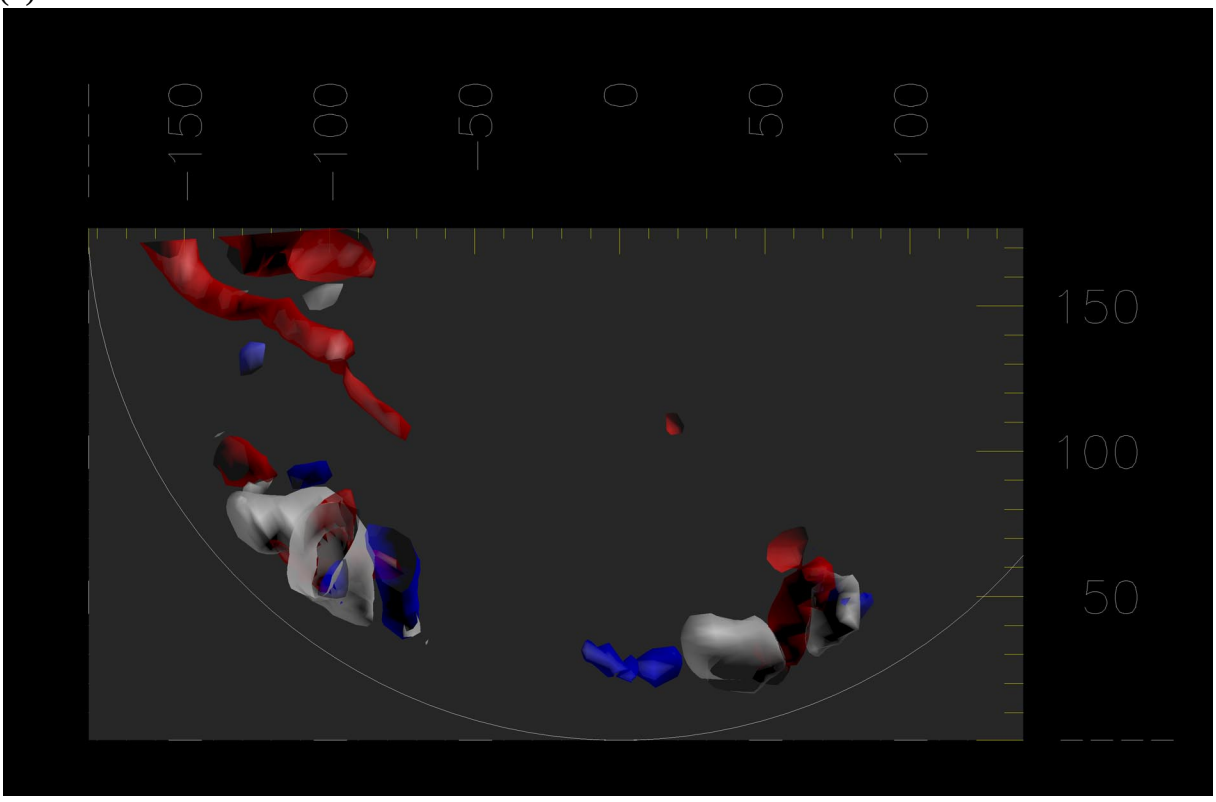

Figure 8: Instantaneous flow structure around the end point of control. (a) bird's-eye view; (b) cross-sectional view around $z^+ = 3700$. Isosurfaces: red, vortex with positive rotation ($Q^+ = -0.025$, $\omega_z > 0$); blue, vortex with negative rotation ($Q^+ = -0.025$, $\omega_z < 0$); white, high production ($P_{rz}^+ = 0.2$). Colors on the wall: magenta, blowing; cyan, suction.